

## Determination and verification of mechanical properties of GFRP filament wound pipes

Michał Krzysztoporski\*, Karolina Paczkowska, Zuzanna Pacholec, Wojciech Błażejowski

Wrocław University of Science and Technology, Faculty of Mechanical Engineering, Department of Mechanics, Materials and Biomedical Engineering, 25 Smoluchowskiego St., 50-370 Wrocław, Poland

\*Corresponding author e-mail: [michal.krzysztoporski@pwr.edu.pl](mailto:michal.krzysztoporski@pwr.edu.pl)

<https://doi.org/10.62753/ctp.2024.04.3.3>

### Abstract

Filament winding is an efficient and versatile manufacturing technique utilised to create lightweight high-strength composite structures. Glass fiber reinforced polymers (GFRP) are widely used in filament winding and can be characterised by high tensile strength, corrosion resistance, and favourable stiffness-to-weight ratios. These properties make GFRP composites suitable for various industries such as aerospace, automotive, marine, and civil engineering. Despite their widespread use, accurately identifying and verifying the mechanical properties of GFRP filament wound structures presents significant challenges. This study addresses these challenges by presenting methods to ascertain and verify the mechanical properties of GFRP filament wound pipes. Commercial pipes from Plaston-P composed of an inner PVC layer and an outer shell of glass fiber roving and mat impregnated with polyester resin were examined. Various mechanical tests were conducted, including tensile, compression, and shear tests, following ASTM standards. This paper describes the steps taken to prepare the specimens required for those tests with a strong focus on reproducing the most representative structure, highlighting potential inaccuracies in parameter identification. Finite element (FE) simulations were performed to verify the obtained parameters, using a nonlinear orthotropic material model with a progressive failure approach. The results showed that the simulated value of the apparent tensile strength of the specimen is 75.94 MPa. The fracture of the element was initiated by failure of the roving-resin layers, which was sudden and brittle. The simulation results were compared with the experimental data obtained from split disk tests according to ASTM D2290. The average apparent tensile stress from the experiment was 80.65 MPa and the specimens failed in a brittle manner. The comparison showed a satisfactory correlation between the simulation and the experiment with a value difference of approximately 6%. The failure mechanism was also identical. It proves that the adopted method of identification allows the mechanical properties to be characterised correctly. Future research will focus on improving the correlation between the simulation and experiment by incorporating parameters to account for delamination and continuous damage of the composite.

**keywords:** filament winding, glass fiber reinforced polymers (GFRP), finite element (FE) simulation, progressive failure analysis, materials testing, split disk test

## Introduction

Filament winding is a highly efficient and versatile manufacturing technique used to produce high-strength, lightweight composite structures. Glass fiber reinforced polymers (GFRP), are often chosen in filament winding applications and offer beneficial mechanical properties such as high tensile strength, corrosion resistance, and good stiffness-to-weight ratios. These characteristics are reasons why GFRP composites are utilised in various industries, including aerospace, automotive, marine, and civil engineering. Despite the widespread use of GFRP in filament winding, accurately identifying and verifying the mechanical properties of these composites remains a significant challenge

Currently, there is a wide variety of different FE models that can be employed to describe filament wound structures (1–5). Filament wound structures differ significantly from composite structures achieved by hand layup. The bands laid down onto the mandrel during the process form regions with different angle configurations and thicknesses across the element. Conducting laminate-based simulations would enforce the testing of numerous laminates for a single component. Therefore, all of the currently available models use a ply-based approach.

In order to correctly ascertain the mechanical properties of the material, the structure of the sample has to be similar to that of the final part. According to that, the most suitable solution would be to use an axisymmetric sample, for example, a pipe or disc. Although there are some standards that allow the use of such samples (6–9), it is impossible to determine all the necessary parameters. On the other hand, the most common procedure that allows all the parameters to be determined is the use of flat samples. It generates technological inconveniences in manufacturing those samples by filament winding. Furthermore, the structure of the composite wound on a flat mandrel is different from that on an axisymmetric core, potentially generating incorrect values of the identified parameters. In the literature, various publications can be found that present different approaches to circumvent this issue, such as using the rule of mixtures, the calibration of parameters with the use of reverse engineering or characterization of the material employing non-standardized methods (10–19). However, all of those approaches have limitations. This paper aims to present an alternative method that utilizes flat samples, which enables the most common standards, in this case ASTM D3039, D6641, D7078 and ISO 527, to be applied. It also includes verification of the established parameters via the split disc test according to ASTM D2290.

## Object of study

The research was carried out on commercial pipe obtained from the Plaston-P company, a manufacturer of plastic reinforced pipelines for various branches of industry, particularly deep coal mines, the refining and

gas industry, metal ore mines, mineral resources, processing plants, and the chemical industry. The examined pipe was produced from PVC pipe which served as the inner layer and also as a mandrel for the outer shell wound from glass fiber roving and glass fiber mat impregnated with polyester resin (Fig. 1). Therefore, it is necessary to identify the parameters of those three materials to conduct an FE simulation.

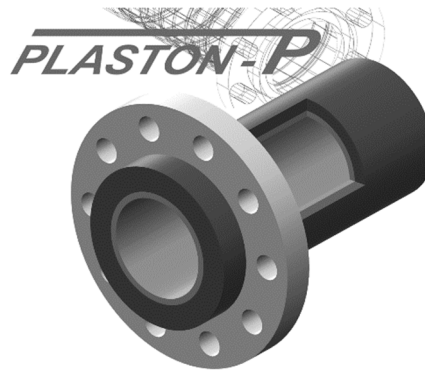


Fig. 1. Plaston-P pipe structure

### Preparation of samples

In order to prepare the specimens for the strength tests, flat plate samples were manufactured. One type of plate was made of glass fiber roving and polyester resin and was manufactured by winding it on a sheet metal plate (Fig. 2). The fibers were aligned in a unidirectional and bidirectional manner. The curing process was conducted under the press. The second type of plate was made of glass fiber mat and polyester resin and manufactured by the hand layup method (Fig. 3). The curing process was also conducted under the press.

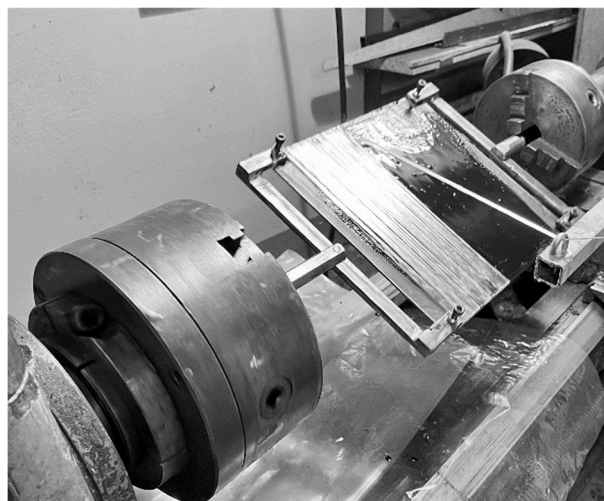


Fig. 2. Winding of flat plate



**Fig. 3. Plate made out of glass fiber mat and polyester resin after hand layup**

The specimens were cut from the plates on a waterjet machine to the dimensions and shapes specified in the standards. For the unidirectional specimens for the tensile and compression test, additional tabs were glued on.

Due to the fact that the PVC layer also must be considered as a laminate layer, its mechanical properties had to be determined. To do this, 20 mm strips were cut axially out of PVC pipe (Fig. 4) and finally shaped on a milling machine (Fig. 5).



**Fig. 4. PVC specimens cut from pipe**

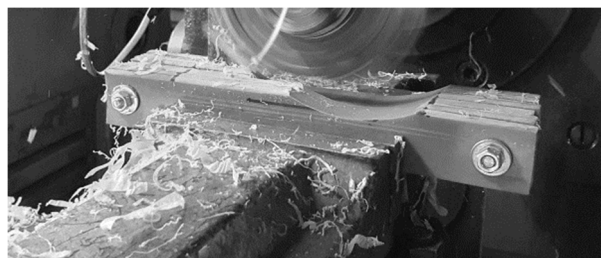


**Fig. 5. PVC specimens shaped on milling machine**

### Determination of mechanical properties

The mechanical properties were determined by means of static tensile, compression, and shear tests. The tensile test was conducted according to ASTM D3039 (Fig. 6). Three sorts of specimens were tested: unidirectional with fibers orientated parallel to the load direction, unidirectional with fibers orientated perpendicular to the load direction, and random-discontinuous fiber orientation. Strain during the test was measured by strain gauges placed in the middle of the specimens, in the parallel and perpendicular directions. For the glass fiber roving and polyester resin composite, orthotropic material properties were determined:

1.  $E_1$  – Young's modulus in the fiber direction
2.  $E_2$  – Young's modulus perpendicular to the fiber direction
3.  $\nu_{12}$  - in plane Poisson's ratio
4.  $X_t$  - maximum tensile stress in the fiber direction
5.  $Y_t$  - maximum tensile stress perpendicular to the fiber direction



Fig. 6 Unidirectional specimen during tensile test

For the glass fiber mat and polyester resin composite, isotropic material properties were determined:

1.  $E$  – Young's modulus
2.  $\nu$  - Poisson's ratio
3.  $X_t$  - maximum tensile stress

To determine the compression strength of the composites, a combined load compression test according to ASTM D6641 (Fig. 7) was performed. Two types of specimens were tested: unidirectional with fibers orientated parallel to the load direction and unidirectional with fibers orientated perpendicular to the load direction. The test results were used to determine:

1.  $X_c$  - maximum compression stress in the fiber direction



2.  $Y_c$  - maximum compression stress perpendicular to the fiber direction

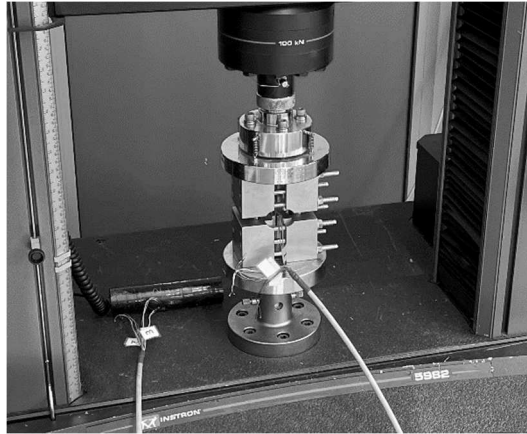


Fig. 7. Unidirectional specimen during compression test

The shear properties of the composite were identified by means of the V-notch rail shear method according to ASTM D7078 (Fig. 8). V-notched specimens with  $[0/90]_s$  laminate were used. Strain during the test was measured by biaxial rosette strain gauges placed in the middle of the specimens. The following parameters were determined:

1.  $G_{12}$  – in plane shear modulus of elasticity
2.  $S_{12}$  – ultimate in plane shear stress



Fig. 8. Specimen during shear test

For the PVC specimens, the tensile test was conducted according to ISO 527-2 (Fig. 9). Strain during the test was measured by extensometers, in the parallel and perpendicular direction. The following isotropic material properties were determined:

1.  $E$  – Young's modulus

2.  $\nu$  - Poisson's ratio
3.  $X_T$  - maximum tensile stress

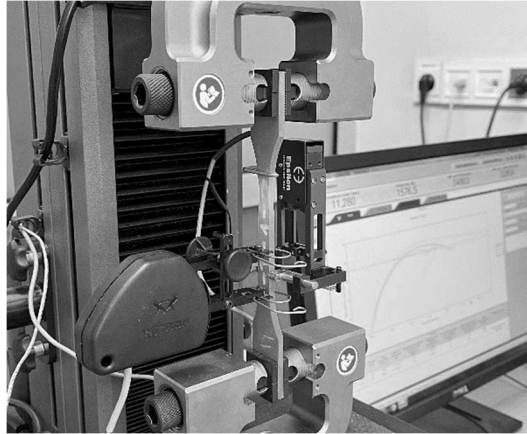


Fig. 9. PVC specimen during tensile test

The exact values of the identified parameters are protected by commercial confidentiality.

### Verification test

To compare a simulation based on the parameters of the individual layers with an experiment using laminate wound on an axisymmetric mandrel, the split disk test was performed according to ASTM D2290. In this test the specimen is subjected to loading via the self-aligning split disk test fixture, which induces tensile stress in the test ring (Fig. 10). Specimen preparation required drilling 18 mm diameter holes in the test tube with 35 mm spacing. Next, the pipe was cut into rings through the centre points of the holes.

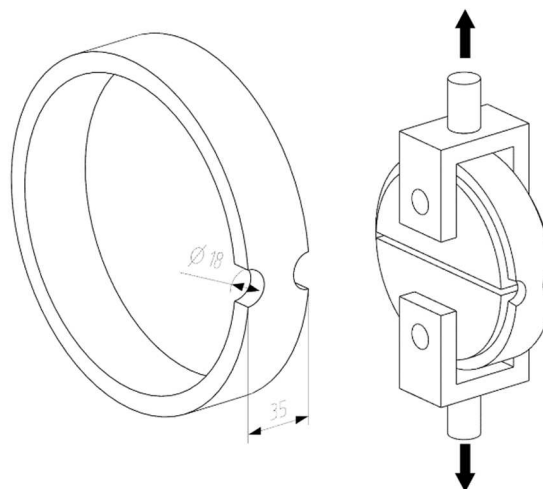
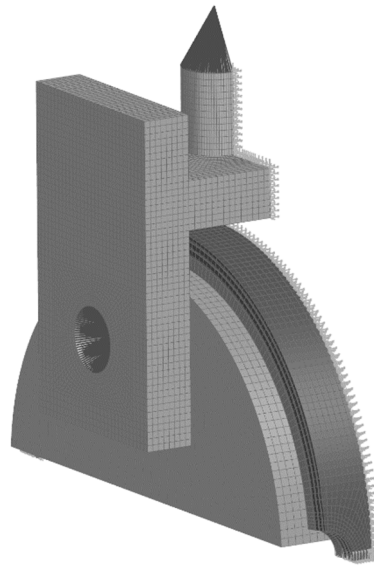


Fig. 10. Scheme of split disc test

Before conducting the experiment, an FE simulation was prepared (Fig. 11). The model shows a quarter of the real geometry using symmetry boundary conditions. The geometry was discretised using linear solid HEXA elements. Nonlinear contact was applied between the inner face of the specimen and the outer face of the split disk. The connection between the clevis and split disk was simplified by using RBE elements connecting the centre points of the holes with the inner nodes of the holes and then connecting the centre points with the BAR element with applied pin cross section properties.



**Fig. 11. FE model of split disc with fixture**

The laminate layers were modelled as separate, perfectly glued meshes. They use non-linear orthotropic material with the parameters described in the previous section. The nonlinearity of the material is simulated by means of the progressive failure approach utilising the maximum stress failure criterion. Failure occurs if one of the following states is reached:

$$X_T \leq \sigma_{11} \text{ or } \sigma_{11} \leq X_C \quad (1)$$

$$Y_T \leq \sigma_{22} \text{ or } \sigma_{22} \leq Y_C \quad (2)$$

$$|\tau_{12}| \geq S_{12} \quad (3)$$

The failed finite element loses 100% rigidity, and the simulation continues until ultimate failure of the specimen. The clevis and split disk model uses linear isotropic material with standard steel properties, such as  $E=210$  GPa and  $\nu=0.28$ .



### Simulation results

The results reveal that in the first part of the simulation the composite behaves linearly. The ultimate failure of the specimen was preceded by short nonlinearity caused by damage in the roving-resin composite layers. After reaching the maximal capacity of this layer, brittle fracture occurs across the full cross section of the specimen. The described results can be depicted as an apparent stress-time graph (Fig. 12). The apparent stress can be calculated using the following equation:

$$\sigma_a = \frac{F}{A_m}, \quad (4)$$

where  $\sigma_a$  is the apparent tensile stress,  $F$  is the applied force to the specimen, and  $A_m$  is the cross section of the specimen.

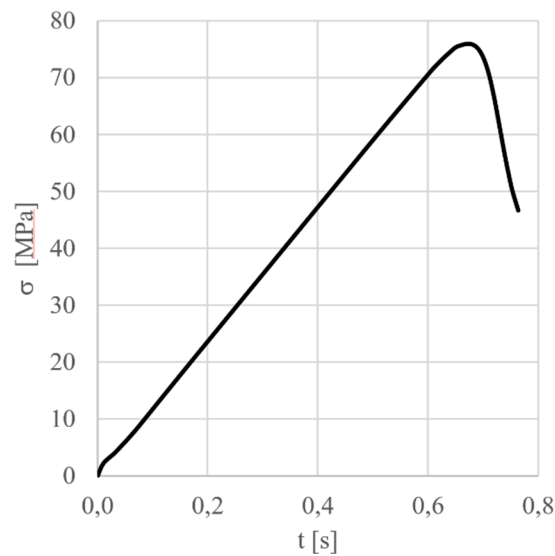
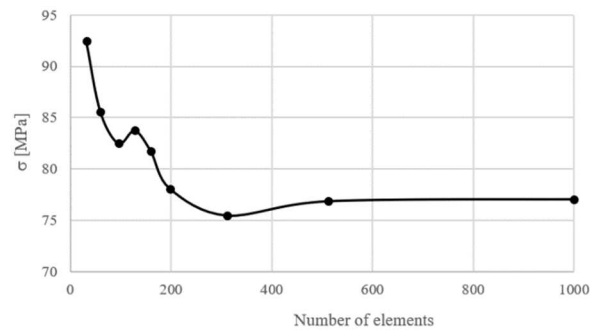


Fig. 12. Apparent tensile stress versus time diagram from FE simulation

To obtain the ultimate failure stress value, a mesh convergence study was conducted. The results are presented in Fig. 13, which illustrates the correlation between maximum stress and number of elements in the region of failure.



**Fig. 13. Results of apparent tensile stress convergence study**

The procedure of changing the number of elements in the region of failure is presented in Fig. 14.

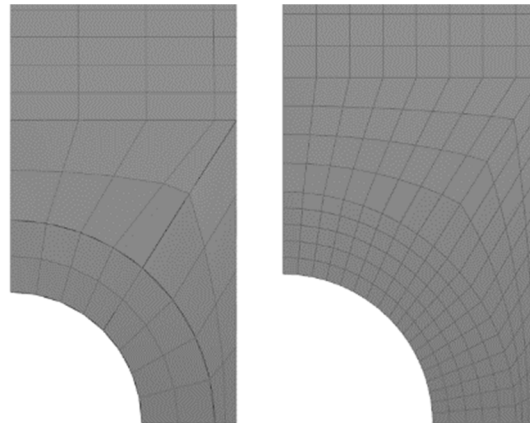


**Fig. 14. Method of changing number of elements in convergence study**

The function converges to the stress of 77.07 MPa, but the lowest value is 75.48 MPa. This is caused by nonlinearities connected with the contact between the specimen and the split disc. Nonlinearities in the material also had a negative influence on the convergence. As the final result of the simulation, the lowest obtained value is used.

## Experiment

The experiment was carried out on an MTS 810 machine. The specimen was mounted on the machine using a custom fixture. The full setup is presented in Fig. 15.

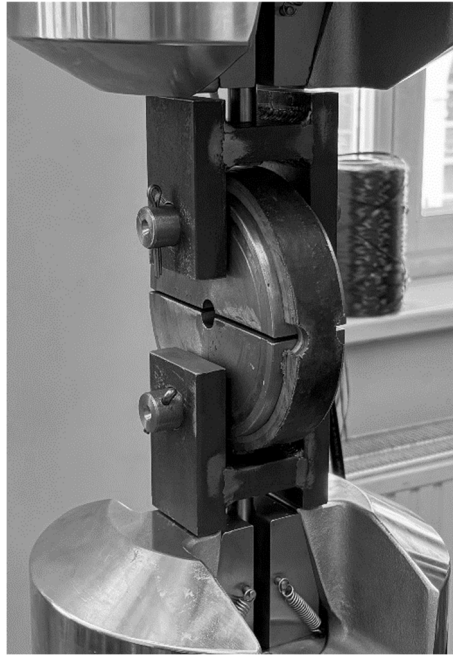


Fig. 15. Sample with fixture mounted on test machine

Five samples were tested, which were loaded at the constant speed of 2 mm/min until failure.

All the samples failed in a sudden and brittle manner, without progressive stiffness degradation. The following tables present a summary of the test results and a comparison between the experiment and the simulation.

Table 1. Summary of test results

Sample	$\sigma_a$ [MPa]
1	84.30
2	80.00
3	83.63
4	78.33
5	77.00
<b>Average</b>	<b>80.65</b>
<b>Standard deviation</b>	<b>3.21</b>
<b>Coefficient of variation</b>	<b>3.98%</b>

Table 2. Comparison of experiment and simulation results

	$\sigma_a$ [MPa]
Experiment	80.65
Simulation	75.94
Difference	4.71
Percentage difference	5.84%

## Conclusions

The paper presented a procedure to determine and verify the mechanical properties of GFRP filament wound pipe. Due to the lack of a standard test that allows the use of axisymmetric specimens, the filaments were wound on a flat mandrel. This allowed standard tensile, compression and shear tests to be conducted according to ASTM standards based on flat samples. All the necessary mechanical properties of the individual layers were ascertained. To verify if they can be used to simulate elements wound on standard axisymmetric mandrels, verification was carried out using the split disc test described in the ASTM D2290 standard. The comparison between the simulation and experimental results showed a satisfactory correlation, which demonstrates that the chosen method can be successfully utilised to simulate these kinds of elements.

The simulation and experiment results differ from each other by about 6%, which indicates a satisfying correlation. The failure mechanism was also predicted correctly, that is, sudden brittle failure of all the plies. The difference between the results can be caused by several factors. Firstly, the band tension distribution on the flat wound plate is different from the distribution on the pipe. This can negatively affect the mechanical properties that were subsequently input for the simulation. Secondly, the maximum stress failure theory, which was used in the progressive failure analysis of the composite material, is reported to be one of the most conservative [10]–[12]. It could also lower the maximum stress value obtained for the simulation compared to the experiment. Moreover, the simplification taken into account in the FE model, that is, transverse isotropy and perfect gluing of the layers, may possibly enlarge the difference between the results.

In future research, it is planned to determine the necessary parameters to take into account delamination and continuous damage of the composite in different directions. It may contribute to improving the correlation between the simulation and experiment.

## REFERENCES

1. Cadfil manual [Internet]. [cited 2023 May 12]. Available from: <https://www.cadfil.com/help/html/cadfil-fea-interface.html>

2. Koussios S. Filament Winding: A Unified Approach. 2004. 404 p.
3. Faria H. Analytical and Numerical Modelling of the Filament Winding Process. 2007;
4. Błażejewski W. Kompozytowe zbiorniki wysokociśnieniowe wzmocnione włóknami według wzorów mołkaych. 2013;
5. Haas J, Aberle D, Krüger A, Beck B, Eyerer P, Kärger L, et al. Systematic Approach for Finite Element Analysis of Thermoplastic Impregnated 3D Filament Winding Structures—Advancements and Validation. *J Compos Sci*. 2022;6(3).
6. ISO Standard. ISO 8521 - Plastics piping systems – Glass-reinforced thermosetting plastics (GRP) pipes and fittings – Test methods for the determination of the initial longitudinal tensile properties.
7. ISO Standard. ISO 7685:2019 Glass-reinforced thermosetting plastics (GRP) pipes — Determination of initial ring stiffness.
8. ASTM Standard. ASTM 2344 Standard Test Method for Short-Beam Strength of Polymer Matrix Composite Materials. *Annu B ASTM Stand*. 2011;00(Reapproved 2006):1–8.
9. ASTM Standard. ASTM 2290-12 Standard Test Method for Apparent Hoop Tensile Strength of Plastic or Reinforced. *ASTM B Stand*.
10. Ojha S, Bisaria H, Mohanty S, Kanny K. Static and dynamic mechanical analyses of E-glass-polyester composite used in mass transit system. *Emerg Mater Res*. 2022;12(1):28–36.
11. Toh W, Tan L Bin, Tse KM, Giam A, Raju K, Lee HP, et al. Material characterization of filament-wound composite pipes. *Compos Struct*. 2018;206(August):474–83.
12. Lin S, Xu L, Li S, Liu X, Jiang W, Jia X. Numerical study of progressive damage analysis on filament wound composite tubes embedded with metal joints. *J Mech Sci Technol*. 2022;36(11):5667–78.
13. Crouzeix L, Moreno HH, Perié JN, Douchin B, Robert L, Collombet F. On the identification of mechanical properties using structural tests and optical methods. *Proc 2006 SEM Annu Conf Expo Exp Appl Mech 2006*. 2006;2:705–14.
14. Charan VSS, Vardhan AV, Raj S, Rao GR, Rao G V., Hussaini SM. Experimental characterization of CFRP by NOL ring test. *Mater Today Proc [Internet]*. 2019;18:2868–74. Available from: <https://doi.org/10.1016/j.matpr.2019.07.154>
15. Perillo G, Vacher R, Grytten F, Sørbø S, Delhaye V. Material characterisation and failure envelope



evaluation of filament wound GFRP and CFRP composite tubes. *Polym Test*. 2014;40:54–62.

16. Henry TC, Bakis CE, Smith EC. Determination of effective ply-level properties of filament wound composite tubes loaded in compression. *J Test Eval*. 2015;43(1):96–107.
17. EL-Wazery MS, EL-Elamy MI, Zoalfakar SH. Mechanical properties of glass fiber reinforced polyester composites. *Int J Appl Sci Eng*. 2017;14(3):121–31.
18. Szabó G, Váradi K, Felhős D. Finite Element Model of a Filament-Wound Composite Tube Subjected to Uniaxial Tension. *Mod Mech Eng*. 2017;07(04):91–112.
19. Zacharakis I, Giagopoulos D, Arailopoulos A, Markogiannaki O. Optimal finite element modeling of filament wound CFRP tubes. *Eng Struct* [Internet]. 2022;253(June 2021):113808. Available from: <https://doi.org/10.1016/j.engstruct.2021.113808>